

Supporting Information

Direct and Sensitive Detection of Mercury in Soil by Portable Electromagnetic Heating Vaporization and Purge-and-trap Followed by Microplasma Optical Emission Spectrometry

Zhengqin Pang,^a Tian Ren,^a Yuanyuan Liu,^a Jiahui Yang,^b Yurong Deng,^{a,*} and Chengbin Zheng^{a,*}

^aKey Laboratory of Green Chemistry & Technology of MOE, College of Chemistry, Sichuan University, Chengdu 610064, P. R. China

^b Analytical & Testing Center, Sichuan University, Chengdu, Sichuan 610064, China

Corresponding Author

Email address: abinscu@scu.edu.cn (C.B. Zheng), yding@scu.edu.cn (Y.R. Deng)

Table of Contents

1. Experimental conditions for HG-AFS

2. Optimization of experimental parameters for μ PD-OES

3. Comparison of the analytical performance of this method with other similar methods

1. Experimental conditions for HG-AFS

Table S1. Experimental conditions for HG-AFS

Conditions	Values
Concentration of HNO ₃ , % (v/v)	5
Concentration of KBH ₄ , % (m/v)	0.01
Concentration of KOH, % (m/v)	0.2
Carrier gas flow rate, mL min ⁻¹	300
Shield gas flow rate, mL min ⁻¹	900
Negative high voltage, V	280
Observation height, mm	8
Lamp current of Hg, mA	30

2. Optimization of experimental parameters for μ PD-OES

Ar gas can serve not only as a carrier gas to transport the analyte from the adsorption tube to the discharge chamber for detection but also as a discharge gas to generate microplasma for PD-OES and sustain its discharge stable. This dual role significantly influences both the transmission efficiency of the analyte and the stability of the microplasma. Therefore, we varied the Ar gas flow rate from 60 to 140 mL min⁻¹ and observed the corresponding changes in mercury signal intensity, as presented in **Fig. S1a**. It is evident from the figure that the signal strength of mercury increased when the Ar gas flow rate ranged from 60 to 80 mL min⁻¹. However, when the flow rate exceeds 80 mL min⁻¹, the signal strength gradually decreased. This phenomenon can be attributed to the weak and unstable excitation ability of the microplasma at low Ar gas flow rate, leading to inefficient analyte transport. Conversely, at higher flow rates, the reduced residence time of the analyte in the PD discharge chamber, resulted in significant dilution and subsequent reduction in signal strength. Hence, 80 mL/min was selected as the optimal discharge carrier gas flow rate in this experiment.

The excitation ability of PD microplasma depends largely on the voltage applied at both ends of the electrode. Therefore, it is necessary to investigate the effect of discharge voltage on mercury signal intensity. In the range of 1.8-3.3kV, the mercury signal intensity changed with the input voltage at both ends of the electrode, and the results are shown in **Fig. S1b**. With the gradual increase of discharge voltage, the signal strength of mercury also gradually increases gradually, reach the maximum value at 2.5 kV, and then gradually decrease. Normally, the energy between the two electrodes increases with the increase of discharge voltage, which enhances excitation ability of the microplasma. However, too high voltage input can also lead to energy instability of the microplasma, which reduces

the signal strength of the analyte. Finally, 2.5 kV was chosen as the optimal discharge voltage condition for this method.

The gap between the two electrodes significantly affects the density and stability of the microplasma, and thus influences the excitation ability of the microplasma. For this reason, we investigated the effect of discharge gap on mercury signal intensity in the range of 1-5 mm. As shown in **Fig. S1c**, the mercury signal intensity gradually increases with the increase of electrode gap. When the electrode gap is 3 mm, intensity of the mercury intensity signal reaches the maximum level. When the electrode gap exceeds 3 mm, the signal intensity gradually decreases. This might be due to the increase the increase of the discharge gap. When the discharge gap exceeds a certain level, the energy of the microplasma starts to become unstable, and the density gradually decrease. This leads to the weakening of the excitation ability of the microplasma. Therefore, 3 mm was chosen as the optimal discharge gap in the following experiments.

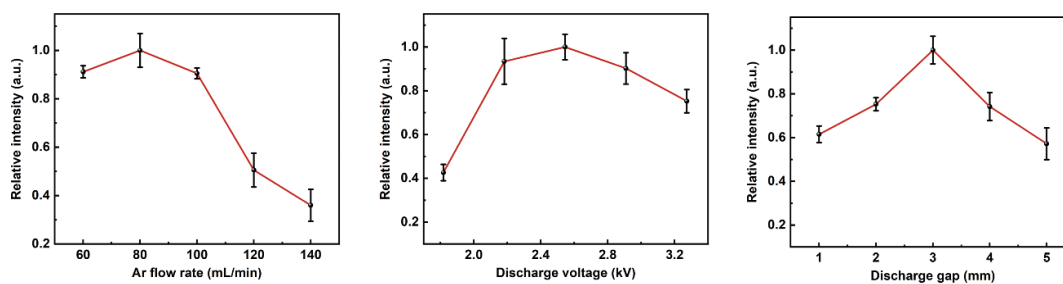


Fig. S1. Effect of (a) Ar flow rate, (b) discharge voltage, and (c) discharge gap on the responses from 240 $\mu\text{g}/\text{kg}$ of Hg.

3. Comparison of the analytical performance of this method with other similar methods

Table S2. Comparison of the analytical performance of this method with other similar methods.

Analysis method	LOD, $\mu\text{g}/\text{kg}$	RSD (%)	Sample	Sample size (mg)	Ref.
EMHV-P&T-PD-OES	0.25/1	3.6/3.8	Soil	60/20	This method
ETV-ICP-MS	LOQ: 3.1	20	Soil	0.5-5.0	1
ETV-Pt/Ni trap AFS	0.4	11	Soil	20	2
ETV-AAS	0.4	4	Soil	50	3
EMHV-DBD-OES	8	11.84	Soil	5	4
ETV-DBD-GT-AFS	0.5	10	Aquatic food	2-12	5
Hg analyzer (gold coil trap)	0.07	15	Food	10	6
DMA-80	2.7	3	Animal tissues	225 \pm 2	7
ETAAS	17	8.3	Sewage sludge	3-30	8
ETV-ICP-MS	0.3	7	Medicinal activated charcoal	1 g	9

References

1. W. Wohlmann, V. M. Neves, G. M. Heidrich, J. S. Silva, A. B. da Costa, J. N. G. Paniz, and V. L. Dressler, *Spectrochim. Acta, Part B*, 2018, **149**. 222-228. <http://doi.org/10.1016/j.sab.2018.08.009>
2. T. Liu, J. Liu, X. Mao, X. Huang, and Y. Qian, *Anal. Chem.*, 2023, **95**. 594-601. <http://doi.org/10.1021/acs.analchem.2c04438>
3. Z. Lv, J. Liu, X. Mao, X. Na, and Y. Qian, *Anal. Chim. Acta*, 2022, **1231**. 340444. <http://doi.org/10.1016/j.aca.2022.340444>
4. X. Liu, K. Yu, H. Zhang, X. Zhang, H. Zhang, J. Zhang, J. Gao, N. Li, and J. Jiang, *Talanta*, 2020, **219**. 121348. <http://doi.org/10.1016/j.talanta.2020.121348>
5. T. Liu, M. Liu, J. Liu, X. Mao, S. Zhang, Y. Shao, X. Na, G. Chen, and Y. Qian, *Anal. Chim. Acta*, 2020, **1121**. 42-49. <http://doi.org/10.1016/j.aca.2020.04.057>
6. B. Wang, L. Feng, X. Mao, J. Liu, C. Yu, L. Ding, S. Li, C. Zheng, and Y. Qian, *J. Anal. At. Spectrom.*, 2018, **33**. 1209-1216. <http://doi.org/10.1039/c8ja00009c>
7. R. F. L. Ribeiro and A. Germano, *Microchem. J.*, 2015, **121**. 237-243. <http://doi.org/10.1016/j.microc.2015.03.005>
8. D. Baralkiewicz, H. Gramowska, M. Kózka, and A. Kanecka, *Spectrochim. Acta, Part B*, 2005, **60**.

409-413. <http://doi.org/10.1016/j.sab.2005.01.010>

9. C.-C. Chen, S.-J. Jiang, and A. C. Sahayam, *Talanta*, 2015, **131**. 585-589.

<http://doi.org/10.1016/j.talanta.2014.08.034>